PNAS RESEARCH ARTICLE | SUSTAINABILITY SCIENCE

Mapped coral mortality and refugia in an archipelago-scale marine heat wave

Gregory P. Asner[a,1], Nicholas R. Vaughn[a], Roberta E. Martin[a], Shawna A. Foo[a], Joseph Heckler[a], Brian J. Neilson[b], and Jamison M. Gove[c]

Contributed by Gregory P. Asner; received December 29, 2021; accepted March 11, 2022; reviewed by Amatzia Genin and Nancy Knowlton

Corals are a major habitat-building life-form on tropical reefs that support a quarter of all species in the ocean and provide ecosystem services to millions of people. Marine heat waves continue to threaten and shape reef ecosystems by killing individual coral colonies and reducing their diversity. However, marine heat waves are spatially and temporally heterogeneous, and so too are the environmental and biological factors mediating coral resilience during and following thermal events. This combination results in highly variable outcomes at both the coral bleaching and mortality stages of every event. This, in turn, impedes the assessment of changing reef-scale patterns of thermal tolerance or places of resistance known as reef refugia. We developed a large-scale, high-resolution coral mortality monitoring capability based on airborne imaging spectroscopy and applied it to a major marine heat wave in the Hawaiian Islands. While water depth and thermal stress strongly mediated coral mortality, relative coral loss was also inversely correlated with preheat-wave coral cover, suggesting the existence of coral refugia. Subsequent mapping analyses indicated that potential reef refugia underwent up to 40% lower coral mortality compared with neighboring reefs, despite similar thermal stress. A combination of human and environmental factors, particularly coastal development and sedimentation levels, differentiated resilient reefs from other more vulnerable reefs. Our findings highlight the role that coral mortality mapping, rather than bleaching monitoring, can play for targeted conservation that protects more surviving corals in our changing climate.

coral bleaching | coral mortality | coral reef | Hawaiian Islands | reef resilience

Significance

Corals exhibit highly variable responses to marine heat waves as well as to local biological and ecological circumstances that moderate them across reef seascapes. This variability makes identifying refugia—reefs possessing conditions that increase coral resilience—nearly impossible with traditional surveys. We developed and applied an airborne coral mortality mapping approach to identify reef refugia in a major marine heat wave across the Hawaiian Islands. A combination of human and environmental factors, including reduced coastal development and lower sedimentation levels, advantaged the majority of refugia over neighboring reefs. High-resolution monitoring of coral mortality reveals a reef geography of both resilience and vulnerability to climate change.

Scleractinian corals, the foundational reef-building organisms of tropical reefs, are under increasing stress from climate change and numerous local and regional stressors (1, 2), with cascading feedbacks on global biodiversity, invaluable ecosystems services, and the livelihoods of millions of people (3, 4). Marine heat waves are a major threat to coral reefs, with 14% of corals lost over the past decade (5) and projected coral losses reaching 90% if climate warming exceeds 1.5 °C (6). Coral refugia, regions of reef possessing conditions that increase climate resilience (7), are possible safe havens from moderate heat waves. Some corals show enhanced resilience through genetics and/or acclimatization (8), while other coral survivors may persist in reef refugia due to environmental factors, such as cooling submarine groundwater discharge along some coastlines (9). While reef refugia are thought to exist (10), they have only been examined at coarse scales of ocean basins (7), and rarely have they been considered within and across reef ecosystems conducive to direct management actions.

Marine heat waves often cause coral bleaching, but bleaching does not necessarily result in coral mortality as many reefs harbor at least some corals that recover and persist following severe heat stress (11). However, most reef survey studies focus on bleaching, a gross indicator of thermal stress during a heat wave. In contrast, fewer studies capture coral mortality, the net effect of a heat wave on reefs. Dead corals are quickly colonized by algal turf and then, by other life-forms, such as macroalgae (12), resulting in a benthic color contrast between live coral and algal surfaces that is more distinct than the continuum of color variation associated with mixtures of live, pale, bleached, and dying corals during a marine heat wave (13). Although previously not possible, the mapping and monitoring of spectral changes associated with coral mortality, rather than coral bleaching, could reveal previously unknown patterns of net coral change.

Quantification of coral mortality across large regions is difficult to achieve due to the vast spatial extent of reefs, great ecological heterogeneity, and measurement barriers associated with traditional coral monitoring methods (14). From a potential refugia standpoint, synoptic high-resolution approaches are needed to quantify net coral change through time to determine reef vulnerability and resilience in the face of global stressors. When coupled with additional information, coral mortality mapping could be used to identify environmental conditions mediating coral responses to heat waves.

Author contributions: G.P.A., N.R.V., B.J.N., and J.M.G. designed research; G.P.A., N.R.V., R.E.M., S.A.F., and J.H. performed research; G.P.A., N.R.V., and J.H. contributed new reagents/analytic tools; G.P.A., N.R.V., and J.H. analyzed data; and G.P.A., R.E.M., S.A.F., B.J.N., and J.M.G. wrote the paper.

Reviewers: A.G., Hebrew University of Jerusalem; and N.K., Smithsonian Institution.

The authors declare no competing interest.

[1]To whom correspondence may be addressed. Email: gregasner@asu.edu.

This article contains supporting information online at http://www.pnas.org/lookup/suppl/doi:10.1073/pnas.2123331119/-/DCSupplemental.

Published May 2, 2022.

The Main Hawaiian Islands (MHI) are spread over more than 1,500 km^2 of the central Pacific Ocean, with reefs experiencing a wide range of human-driven pressures that greatly affect reef resilience (15). The marine heat waves of 2015 and 2019 nonuniformly engulfed the MHI, with the 2015 event generating live coral losses exceeding 50% along some islands but with unmeasured geographic patterns of loss or resistance (16). While the severity of the 2019 heat wave was far less than that experienced in 2015, some reefs did undergo high levels of thermal stress (e.g., 15° heating weeks) and a wide spectrum of bleaching responses from <1 to >30% of coral cover (17).

The 2019 Hawai'i marine heat wave occurred from July to October, providing an opportunity to assess archipelago-scale coral mortality and resistance following a marine heat wave (17). We applied a high-resolution reef mapping approach based on airborne imaging spectroscopy (18) to assess net changes in live coral cover surveyed in January 2019 and again in January 2020. We quantified absolute and relative coral loss across six islands and identified coral reef refugia showing resilience to heating. We combined maps of coral change with mapped environmental factors to assess mediators of coral loss and retention. Our research represents a spatially explicit assessment of coral mortality and refugia following a large-scale marine heat wave.

Results

We mapped a total of 21,773 ha of reef to 16-m depth, which harbored an average of 22.7% (pixel-level SD = 15.8%) live coral cover in January 2019 before the marine heat wave (Table 1). Following the heat wave, a remapping of the same reef area revealed an absolute loss of live coral cover averaging 6.3% (pixel SD = 8.5%). Absolute coral cover losses were unevenly distributed by island and along the coasts of each island (Fig. 1*A* and Table 1). Lana'i underwent the highest levels of absolute coral loss (9.9%; SD = 12.6%), and O'ahu had the least amount of coral loss (5.3%; SD = 7.2%).

Accounting for preheat-wave coral cover, the ecological pattern of relative coral mortality was much different from that of absolute mortality (Fig. 1*B*). Mean relative coral loss was 26.1% (pixel-level SD = 28.4%) across the entire study region but was elevated around Lana'i, Hawai'i, and Kaho'olawe islands, averaging 28.3 to 30.1% (Table 1). This pattern was in accordance with the footprint of the marine heat wave, which was maximum around Lana'i, Kaho'olawe, and the west coast of Hawai'i Island (*SI Appendix*, Fig. S1).

We assessed the absolute and relative effects of the marine heat wave on live coral cover alongside numerous potential

Table 1. Island-scale mean and pixel-level SD (2-m resolution) of coral mortality following the 2019 marine heat wave

Island	Mapped area (ha)	Starting live cover (%)	Absolute loss (%)	Relative loss (%)
Hawai'i	5,354	20.8 (14.1)	6.1 (7.5)	30.1 (28.8)
Maui	5,432	23.8 (14.9)	6.1 (8.3)	23.3 (27.0)
Kaho'olawe	469	22.5 (17.6)	7.3 (9.6)	29.9 (29.5)
Lana'i	1,495	30.2 (22.5)	9.9 (12.3)	28.3 (28.0)
Moloka'i	4,863	23.8 (18.0)	6.4 (8.9)	25.1 (27.8)
O'ahu	4,160	18.9 (12.4)	5.3 (7.2)	25.7 (30.8)
Combined	21,773	22.7 (15.8)	6.3 (8.5)	26.1 (28.4)

Absolute loss is the change in percentage cover of live coral between years, and relative loss is calculated as [2019 − 2020]/2019 of live coral cover. SD = standard deviation

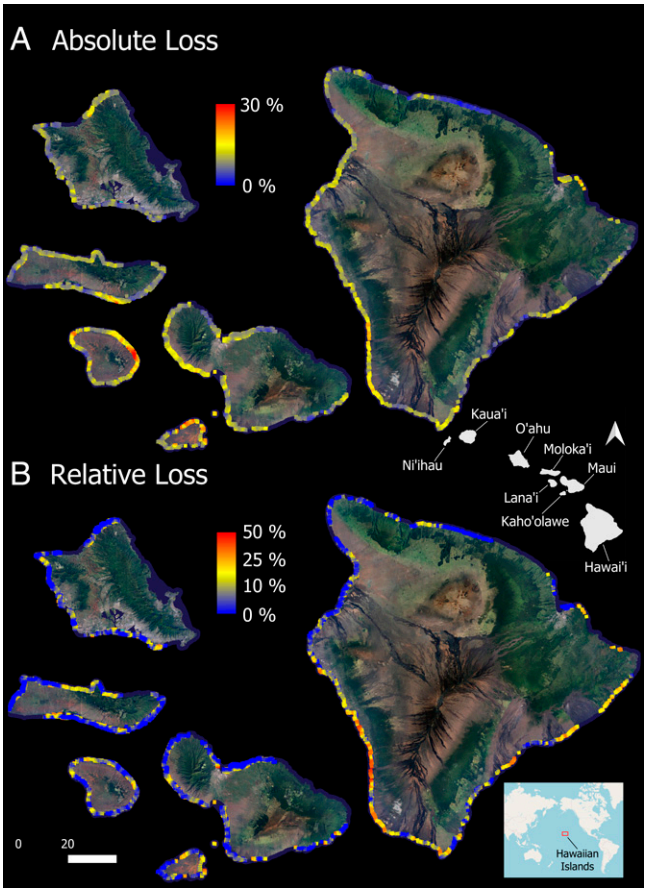

Fig. 1. (*A*) Absolute and (*B*) relative loss in coral cover between January 2019 and January 2020 at 2-m spatial resolution to 16-m water depth. *Lower Right Inset* indicates location of the Hawaiian Islands in the Pacific Ocean. *Middle Right Inset* indicates the geographic distribution of the main eight islands. Absolute loss is reported as percentage cover change between years, and relative loss is calculated as [2019 − 2020]/2019 of coral cover. Sections of coastline with dark blue color were not mapped due to rough sea surface conditions in 2020.

interacting factors (*SI Appendix*, Tables S1 and S2). Because marine heat waves differ in vertical structure and intensity, we first focused on coral mortality by water depth to define the vertical thickness of the thermal anomaly in biological terms (Fig. 2). In absolute cover terms, the 2019 marine heat wave caused the most coral mortality in the 1- to 9-m-depth range, with the greatest loss of 13% observed on Lana'i at 3- to 7-m depth (Fig. 2*A*). In relative cover terms, however, peak losses occurred in the 1- to 4-m-depth range (23 to 63% coral loss), with Kaho'olawe most impacted (Fig. 2*B*). Moreover, relative coral losses remained high at 20 to 35% to our maximum mapping depth of 16 m, indicating that the biologically defined depth of the heat wave exceeded our mapping depth. In situ temperature sensors indicated that the thermal anomaly was about 2 °C down to ∼30-m depth.

Analyses using computational machine learning revealed the key factors that were spatially correlated with absolute and relative coral losses from the marine heat wave (Fig. 3). The severity and duration of the heat wave, as measured in degree heating weeks (DHW), were highly correlated with absolute coral loss (Fig. 3*A*). Solar irradiance, as measured via photosynthetically active radiation (PAR), was a covariate with DHW. Elevated PAR induces additional stress on corals with respect to their algal symbiont, particularly during anomalous temperature events (19). The factors most influential in explaining absolute coral

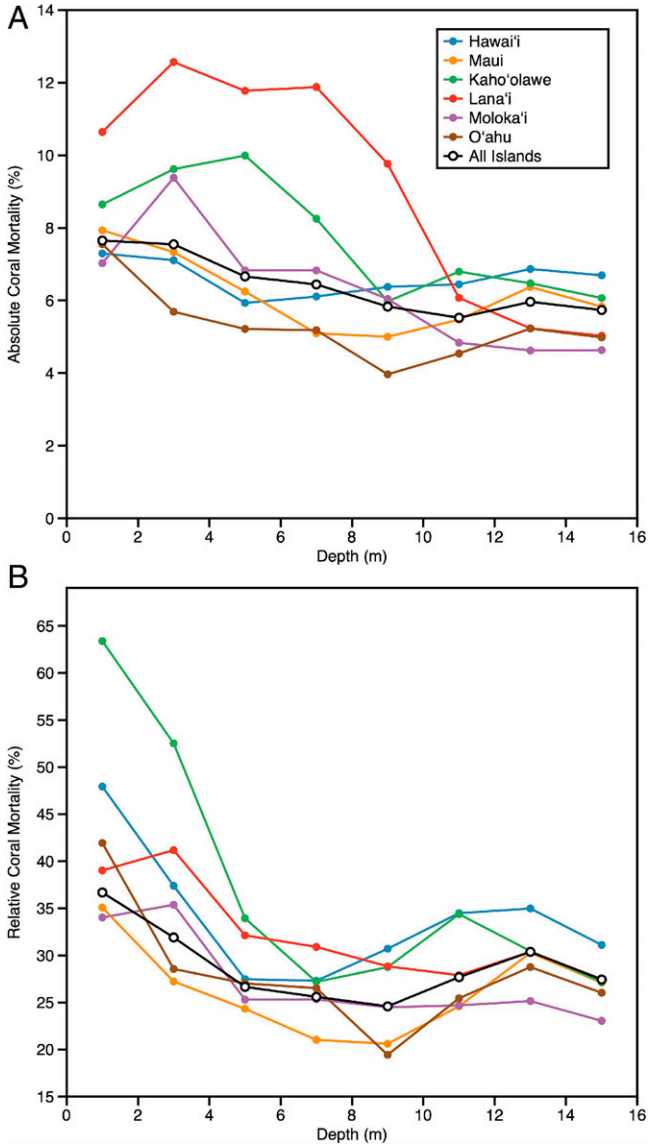

Fig. 2. (*A*) Absolute and (*B*) relative loss in coral cover from 2019 to 2020 by island and seawater depth.

losses were highly variable by island (*SI Appendix*, Fig. S2*A*). Very few of the factors were important for more than any two of the islands, and none were dominant for all individual islands. This suggests that heat-induced coral mortality was highly dependent on local reef-scale factors, despite widespread thermal and light stress in 2019.

A pivotal finding was that the strongest predictor of relative coral mortality across the study region was preheat-wave coral cover (Fig. 3*B*). Specifically, some reefs with higher coral cover before the heat wave fared much better than those with lower cover, suggesting that high-cover reefs may be serving as long-term coral refugia in heat waves. This finding also held for each island individually (*SI Appendix*, Fig. S2*B*). While proportional losses of any quantity can vary inversely with its starting value, high coral cover is not simply a systematic predictor of relative coral loss. Instead, the machine learning approach detected this inverse relationship in a geospatial pattern that was interpretable in specific locations, revealing potential coral refugia.

To further assess this possibility, we analyzed the top 10 live coral cover reefs in the MHI as previously mapped (18) (*SI Appendix*, Table S3). We calculated coral loss on these reefs and compared it with 10 km of adjacent reefs in both directions away from each potential refugium. Our analysis indicated 30 to 40% greater coral survivorship on 7 of the 10 potential refugia (Table 2). The remaining three reefs performed similarly (−6 to +8%) to surrounding nonrefugia. Analyses of potential explanatory variables indicated that less sedimentation and coastal development were correlated with the higher performance of most coral refugia relative to surrounding areas (r = 0.44 to 0.46) (*SI Appendix*, Table S4). However, our analyses did not include a potentially important factor of cool subsurface groundwater discharge that may provide additional protection (9). Despite these refugium-scale findings, we also observed that heat wave–driven coral losses were highly heterogeneous within each reef (Fig. 4). Other than the natural spatial pattern imparted by reef hard-bottom substrate on coral cover, there was no coherent spatial pattern found in the within-reef response of corals to the heat wave.

Discussion

Our study highlights the unique role that coral mortality mapping can play in support of reef conservation and management as ocean climate continues to change. Whether in a laboratory or field setting, understanding which corals bleach is important for assessments of heat and light stress response. However, coral morality mapping provides an avenue to determine net rates of coral loss over large areas, which reveal ecosystem-level resilience.

Maps of coral mortality following marine heat waves and other disturbances provide input to the growing field of coral reef restoration, which must grapple with numerous issues that limit reef recovery efforts (20, 21). Given the pronounced limitations of carrying out coral restoration at large scales, more tactical approaches are urgently needed to identify areas of both heightened coral mortality and survivorship. Coral mortality mapping can focus subsequent effort on moderately impacted reefs that might benefit from direct interventions while avoiding areas of severe decline that may prove fruitless in restoration efforts. Still other reefs showing resilience can be identified and designated for protection. These types of emergent options could help manage enormous areas, such as the Great Barrier Reef (22).

While we found reefs with elevated coral resilience to the 2019 marine heat wave, pronounced within-refugium heterogeneity of coral mortality was also observed. This may be an indicator of genetic variability in thermal tolerance within and between coral species (23). Such complex spatial patterns of coral performance may, therefore, provide options for the selection of thermally tolerant corals for study. Subsequent selective propagation, based on within-refugium coral performance in heat waves, can help managers and conservationists to enhance reef resiliency by strengthening the pool of genotypes used for restoration.

Our airborne results reveal a highly complex geography of coral vulnerability to thermal events at individual reef to archipelago scales. While high temperature and light stress remain broad forces of coral mortality, the scale dependence of coral loss and survivorship is far more complex than can be accounted for by these drivers alone. In the 2019 Hawai'i marine heat wave, a range of coral mortality levels was observed, and on some reefs in areas of less coastal development and lower land to sea sedimentation, corals performed better than in other areas lacking these land-based impacts. Such results point to the need for management to directly address land–reef issues in a changing climate. Despite this understanding, we still lack nearshore maps of subsurface groundwater

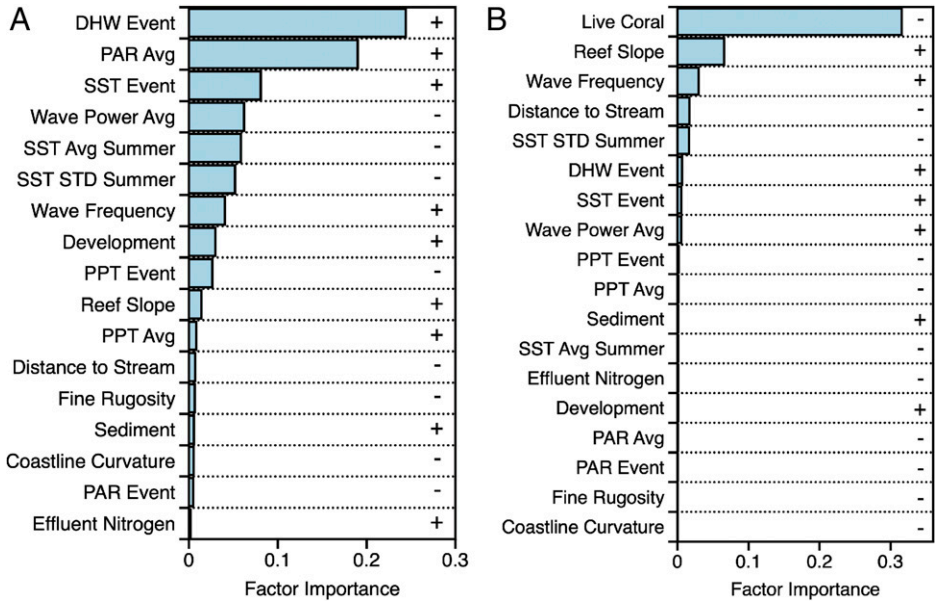

Fig. 3. Importance of factors associated with the spatial pattern of (*A*) absolute and (*B*) relative coral loss for all islands during the 2019 marine heat wave. Plus (+) and minus (−) symbols indicate the direction of the relationship between each mapped factor and coral mortality. Avg = average; STD = standard deviation; PPT = precipitation; SST = sea surface temperature. *SI Appendix*, Fig. S2 shows similar data by island.

discharge, currents, and internal waves, all of which may greatly affect coral outcomes in a warming climate (24, 25). Because preexisting live coral cover was a strong predictor of coral resilience in the 2019 marine heat wave, it may be the case that some of these unmapped factors are supporting coral survival. In fact, mapping coral persistence may provide a way to identify where these factors are biologically relevant.

Coral resilience results from a combination of genetic thermal tolerance (26) and mediating factors, such as human stressors and local hydrodynamics (18). Yet, these interacting factors remain extremely difficult to constrain via traditional studies. Repeat coral mortality mapping could be integrated with laboratory and field-based approaches to better understand options and to drive efforts at scales of greater ecological efficacy. While the remote sensing with imaging spectroscopy used here is currently only available via a few airborne platforms, space-based systems are in rapid development (27), which will make coral mortality mapping routine in a few years. The discovery and monitoring of coral reef refugia offer an important pathway for meaningful conservation interventions that protect more corals in our changing climate.

Methods

Airborne Data Collection. In January 2019, we collected and generated live coral cover maps for the MHI at 2-m spatial resolution using the Global Airborne Observatory (GAO) (18, 28). The mapping process was repeated in January 2020. Repeat coverage was obtained for the islands of Hawai‘i, Kaho‘olawe, Lana‘i, Maui, Moloka‘i, and O‘ahu to a depth of 16 m. Details of the mapping campaigns, including instrumentation, data processing, and field verification, are in *SI Appendix*.

Island-Level Coral Mortality. We computed average coral loss values, in both absolute and relative terms, for each island. Absolute coral loss was the change in percentage cover of live coral between years, and relative loss was calculated as [2019 − 2020]/2019 of live coral cover. Subsequent analyses included pixels containing hard-bottom substrate, defined using 2019 sand cover maps by setting a maximum sand cover threshold of 50% and a minimum of 50% of combined live coral cover, algal cover, and bare rock. In a previous study, we identified the top 10 highest average coral cover reefs across the MHI (18) (*SI Appendix*, Table S3). We assessed whether such high live coral regions had higher coral survivorship than surrounding coastlines following the marine heat wave to investigate the existence of reef refugia. We computed average absolute and relative coral loss values for

Table 2. Coral loss in the top 10 highest live coral cover reefs identified in ref. 18 compared with neighboring reefs

	Potential refugium (%)		Neighboring reefs (%)		
Name	Cover loss	Relative loss	Cover loss	Relative loss	Refugium/neighbor, ratio of relative loss (%)
Hawai‘i: Kīholo	7.0 (9.8)	18.1 (24.2)	6.1 (7.6)	27.4 (29.2)	−34
Hawai‘i: Keawaiki	7.1 (9.0)	19.4 (24.4)	6.1 (7.5)	27.6 (28.9)	−30
Hawai‘i: ‘Anaeho‘omalu	6.3 (9.1)	19.4 (25.5)	6.1 (7.6)	27.6 (29.0)	−30
Hawai‘i: Keaukaha	7.1 (9.8)	17.4 (25.6)	6.0 (8.7)	29.0 (36.8)	−40
Hawai‘i: Pāpā Bay	6.4 (7.4)	27.6 (27.1)	8.1 (7.9)	41.5 (30.9)	−33
Lana‘i: East	16.1 (15.9)	26.8 (25.7)	7.9 (9.9)	28.6 (30.2)	−6
Hawai‘i: Makako	7.9 (8.3)	31.4 (29.4)	6.3 (7.3)	29.1 (29.2)	+8
Maui: Ka‘anapali South	8.2 (10.5)	25.5 (29.9)	7.3 (9.2)	27.6 (29.8)	−8
Southeast Moloka‘i	8.9 (12.1)	20.0 (26.2)	7.3 (9.1)	31.8 (30.7)	−37
Hawai‘i: Wai‘olena	6.9 (8.5)	19.9 (25.4)	6.0 (8.7)	28.7 (36.7)	−31

Absolute loss is the change in percentage cover of live coral between years, and relative loss is calculated as [2019 − 2020]/2019 of coral cover.

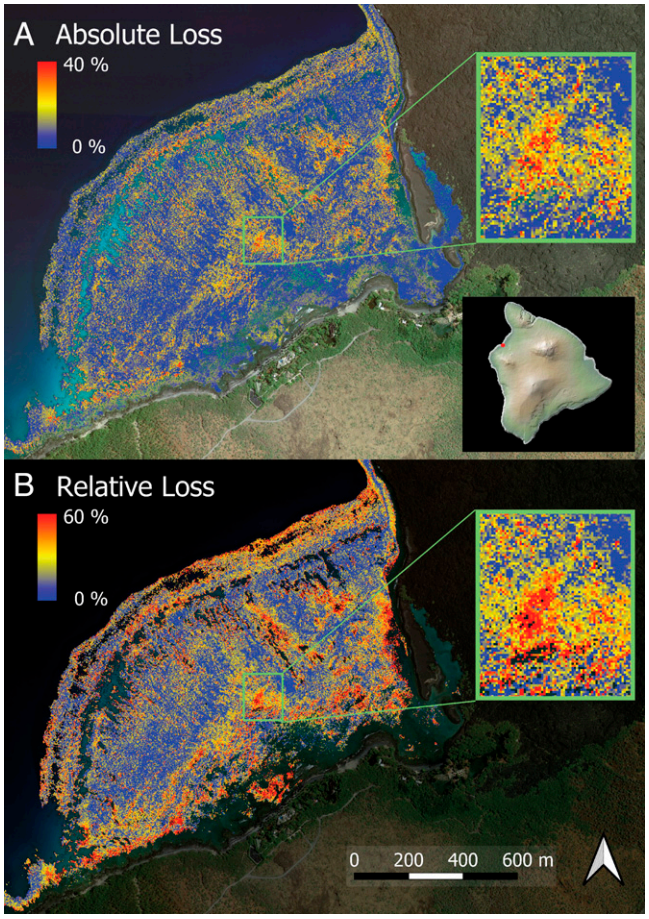

Fig. 4. Example full-resolution mapping of (*A*) absolute and (*B*) relative loss in coral cover between January 2019 and January 2020 at 2-m spatial resolution to 16-m water depth. Absolute loss is reported as change in percentage cover between years, and relative loss is calculated as [2019 − 2020]/2019 of coral cover. The area shown is Kīholo Bay, Hawai'i Island, a top coral refugium determined in this study (Table 2). *Insets* in *A* include a zoom-in to a subset of the absolute coral loss data at full resolution (upper box) as well as a map of Hawaii Island (lower box) indicating the location of this example. *Inset* in *B* provides a zoom-in to a subset of the relative coral loss data at full resolution.

each of the potential refugia as well as for the coastline surrounding each region within a 20-km buffer (10 km to each side of the proposed refugium).

Potential Driver Maps. To assess spatial correlation of mapped live coral loss (2019 to 2020) and spatially variable socioenvironmental drivers, we compiled 19 potential driver maps for each of the islands (*SI Appendix*, Table S2). Two potential drivers were generated from GAO bathymetry maps derived from the 2019 airborne Visible to Shortwave Infrared data collection (29): 2-m resolution rugosity (*Fine Rugosity*) using a methodology defined in ref. 30 and seafloor slope (*Reef Slope*) computed on benthic depth maps averaged to 6-m resolution. Three maps of coastal geometry were created using a vector map of the coastlines of the MHI downloaded from the State of Hawai'i Office of Planning (https://planning.hawaii.gov/gis; accessed June 2020). We measured coastline complexity at each vertex in the coastal outline by summing the absolute angles (in radians) at all vertices within 200 m of the given vertex and dividing by the number of vertices used in the sum. We then created a raster map of coastline complexity (*Coastline Curvature*) by interpolating the vertex complexity values using inverse distance weighted averaging with a power of two. In addition, we developed an algorithm to identify all embayments (concave regions of coastline) that span up to 2 km in width. From these identified embayments, we set up a 10-m grid for each island and computed the distance inside the embayment for each pixel in the grid (*Embayment Distance*). Pixels outside of identified embayments were given an *Embayment Distance* of zero. In some embayments, we noticed that corals near the bay shoulder survived better than those near the bay head. To quantify *Embayment Position*, we created a metric that takes the value of one at the head (most interior part of the bay) and the value of zero at the shoulder (most outward point) of an embayment, with other points assigned a value from zero to one. This metric was computed using two values: 1) distance inside an embayment relative to maximum distance in the given embayment (*rdist*) and 2) distance along the segment connecting the two shoulders (referred to as "stretch" in *SI Appendix*, Fig. S1) relative to the total distance of this stretch (*rstretch*). With these two relative values, *Embayment Position* was computed as $0.5(1 + rdist) + \mid rstretch - 0.5 \mid$ for each pixel on the same grid used for mapping *Embayment Distance*.

To incorporate information about the water temperature before and during the 2019 warming event, we incorporated daily sea surface temperature (SST) maps available from National Oceanic and Atmospheric Administration (NOAA) Coral Reef Watch (https://coralreefwatch.noaa.gov/). Daily CoralTemp v3.1 blended SSTs are derived from multiple satellite sensors maps and validated against a network of temperature sensors (31, 32). A moving average SST was computed using a 7-d window on daily SST maps. For each year, the summer period was defined as 45 d before and after the date on which the maximum value of this moving average SST was achieved. We computed the mean and SD of the moving average SST for all days within the summer period for each year. The mean of the annual means (*SST Avg Summer*) and the mean of the annual SDs (*SST STD Summer*) were recorded as inputs into the driver analysis to define recent patterns of temperature fluctuation. We also computed the maximum 7-d moving average SST achieved during the 2019 warming event, defined as the period from 1 August to 31 December (*SST Event*), as an indicator of maximum instantaneous heat stress. We calculated DHW as an indicator of accumulated heat stress. DHW is computed from weekly maximum temperature maps in a moving 12-wk window by comparing the weekly maximum against an average maximum summer SST value for the same area. All positive (warmer than average) differences between the weekly maxima inside the 12-wk window and the average maximum summer SST are summed. We used the maximum DHW value measured during the 3-mo 2019 warming event (*DHW Event*) as a metric of accumulated heat stress. For all the above maps, pixels containing water depths less than 30 m were removed prior to averaging due to noise artifacts that commonly occur in shallow waters (33). Values for pixels in shallow water were computed using nearest neighbor interpolation on the deeper water pixels.

Because solar radiation has been shown to be correlated with coral bleaching damage (34, 35), we compiled maps of 8-d PAR from Coral Reef Watch at 750-m resolution. These maps indicate the amount of radiation reaching the water surface during the given time period and depending on turbidity, the amount of radiation reaching the ocean floor. From these data, we compiled a map of average PAR from 2012 to 2019 (*PAR Avg*) and a map of maximum PAR observed during the 2019 marine heat wave (*PAR Event*). The PAR maps were filtered to remove shallow water pixels in the same manner as the SST and DHW maps.

To test the degree to which terrestrial input into the ocean via surface and groundwater interacts with warming waters on coral loss, we used a vector layer of streams also obtained from the Hawai'i Office of Planning website. We generated a map of the distance to stream inlets (*Dist. to Stream*) by directly computing the distance from each pixel on the grid to the nearest stream. We downloaded monthly total precipitation map data, as measured by the Global Precipitation Mission satellite constellation (36) at 0.1° (∼10-km) resolution, and created two maps: the total terrestrial precipitation during all of 2019 (*PPT Avg*) and the total precipitation occurring during the warming period (*PPT Event*). These maps were used as an alias for the total freshwater flow into the ocean. Nearest neighbor interpolation was used to interpolate terrestrial precipitation seaward from the coast. We next included a layer of modeled sediment export available from the Ocean Tipping Points Project (15, 37) as an indicator of how much sedimentation could be expected to affect water clarity and light transmission (*Sediment*).

Two metrics of human activity–related inputs into the ocean were also available as layers from the Ocean Tipping Points Project. First, a *Development* layer of land use changes from natural landscape to human-built environments during 2005 to 2010 was included to identify impacts of coastal development on live coral. Next, as nutrient leaching from on-site sewage systems can increase algal growth in downstream waters and have direct impacts on coral physiology, we included a layer of estimated "nitrogen flux" (*Effluent Nitrogen*) (15, 37, 38) in the driver analyses.

Finally, wave forcing is another factor often linked with coral health; thus, we used wave power maps available from the Ocean Tipping Points Project as drivers in the analysis. For these maps, maximum wave power was estimated on a daily basis during the years 2000 to 2013 using a computer model incorporating wind conditions and digital surface maps to model wave spatial patterns

(15, 39). The daily maxima were averaged within each month across all years, creating typical monthly values that were used to detect anomalies as daily maxima that exceed their typical monthly values. We incorporated two layers that quantify the long-term patterns in such anomalous wave forcing into the analysis: the average power of these anomalous waves (*Wave Power Avg*) and the average annual frequency of anomalous waves (*Wave Frequency*).

Driver Analyses. We used random forest machine learning (RFML) models (40) to assess the importance and pattern of influence of each of the potential drivers on the amount of coral lost both as absolute (percentage) cover lost and as relative cover lost from the starting live cover in 2019. RFML regression models are flexible and nonparametric, allowing for complex interactions between input factors to be mapped out using an array of individually fit regression trees. Predictions are computed from averaged predictions across the individual regression trees. Built-in automatic pruning of each tree and fitting with bagged samples reduce overfitting. The RFML models were created at two different scales to identify changes in importance between the different scales. The first scale was archipelago, in which samples from all islands were combined into a single RFML model. At a second full-island scale, a separate RFML model was built for each of the six study islands.

Prior to analysis, the live coral loss maps were down sampled to 100-m spatial resolution by averaging the 2-m values for all areas where at least 30% of the 2-m pixels contained valid, unfiltered values. The individual driver maps were also down sampled using pixel averaging or up sampled using a cubic spline algorithm to match the 100-m grid of the loss maps. Training data for each island were taken from all 100-m resolution pixels that had valid values across map layers.

Modeling was carried out using the Scikit-Learn Python package (41). For each RFML model, a full grid search was performed to find the optimal metaparameters for the model. Metaparameters that were allowed to vary were 1) the number of estimators (regression trees), 2) the minimum number of samples at each tree leaf node, and 3) the maximum depth (number of recursive splits) allowed for each tree. A model was fit with fivefold cross-validation for each combination of metaparameters, and the optimal metaparameters were determined from the combination that produced the lowest mean square error. The optimal parameters were then used to fit a model to the full dataset (no cross-validation). The R^2 value for the predictions of this full model against the observed coral loss values was recorded for later use.

To assess the importance of each driver variable in each model, an R^2 reduction permutation importance metric was computed. For each input variable for each of five iterations, the values for this variable were randomly shuffled, keeping the values of all other variables intact. Model predictions were performed using the permuted dataset, and we retained the difference between the original R^2 and the R^2 computed from this permutation. The five difference values were averaged for each variable to get a single importance value, where larger positive values indicate greater reduction in R^2 and equivalently, greater variable importance.

Data Availability. Mapping data have been deposited in Zenodo (https://zenodo.org/record/4777345) (42).

ACKNOWLEDGMENTS. This study was primarily funded by Lenfest Ocean Program of Pew Charitable Trusts Grant 34039. Key additional support was provided by the NOAA Pacific Islands Fisheries Science Center. This is also a product of the Hawaii Office of Coastal Zone Management Program, pursuant to National Oceanic and Atmospheric Administration Award NA17NOS4l90102, funded in part by the Coastal Zone Management Act of 1972 as amended administered by the Office for Coastal Management, National Ocean Service, National Oceanic and Atmospheric Administration, US Department of Commerce. The GAO is managed by the Center for Global Discovery and Conservation Science at Arizona State University. The GAO is made possible by support from private foundations, visionary individuals, and Arizona State University. The views expressed herein are those of the authors and do not necessarily reflect the views of NOAA or any of its subagencies.

Author affiliations: [a]Center for Global Discovery and Conservation Science, Arizona State University, Hilo, HI 96720; [b]Department of Land and Natural Resources, Division of Aquatic Resources, Honolulu, HI 96813; and [c]Pacific Islands Fisheries Science Center, National Oceanic and Atmospheric Administration, Honolulu, HI 96818

1. T. P. Hughes *et al.*, Global warming and recurrent mass bleaching of corals. *Nature* **543**, 373–377 (2017).
2. R. R. Carlson, S. A. Foo, G. P. Asner, Land use impacts on coral reef health: A ridge-to-reef perspective. *Front. Mar. Sci.* **6**, 562 (2019).
3. F. Moberg, C. Folke, Ecological goods and services of coral reef ecosystems. *Ecol. Econ.* **29**, 215–233 (1999).
4. S. Grafeld, K. L. L. Oleson, L. Teneva, J. N. Kittinger, Follow that fish: Uncovering the hidden blue economy in coral reef fisheries. *PLoS One* **12**, e0182104 (2017).
5. G. C. R. M. Network, "The Sixth Status of Corals of the World: 2020 Report" (Rep., 2021). https://gcrmn.net/2020-report/. Accessed 3 March 2022.
6. IPCC, *Summary for Policymakers* (World Meteorological Organization, Geneva, Switzerland, 2018).
7. G. Keppel, J. Kavousi, Effective climate change refugia for coral reefs. *Glob. Change Biol.* **21**, 2829–2830 (2015).
8. S. L. Coles, B. E. Brown, Coral bleaching–capacity for acclimatization and adaptation. *Adv. Mar. Biol.* **46**, 183–223 (2003).
9. G. Kim, J.-S. Kim, D.-W. Hwang, Submarine groundwater discharge from oceanic islands standing in oligotrophic oceans: Implications for global biological production and organic carbon fluxes. *Limnol. Oceanogr.* **56**, 673–682 (2011).
10. C. Cacciapaglia, R. van Woesik, Reef-coral refugia in a rapidly changing ocean. *Glob. Change Biol.* **21**, 2272–2282 (2015).
11. J. P. W. Robinson, S. K. Wilson, N. A. J. Graham, Abiotic and biotic controls on coral recovery 16 years after mass bleaching. *Coral Reefs* **38**, 1255–1265 (2019).
12. T. R. McClanahan, Primary succession of coral-reef algae: Differing patterns on fished versus unfished reefs. *J. Exp. Mar. Biol. Ecol.* **218**, 77–102 (1997).
13. J. Li, N. S. Fabina, D. E. Knapp, G. P. Asner, The sensitivity of multi-spectral satellite sensors to benthic habitat change. *Remote Sens.* **12**, 532 (2020).
14. T. Kutser, J. Hedley, C. Giardino, C. Roelfsema, V. E. Brando, Remote sensing of shallow waters: 0A 50 year retrospective and future directions. *Remote Sens. Environ.* **240**, 111619 (2020).
15. L. M. Wedding *et al.*, Advancing the integration of spatial data to map human and natural drivers on coral reefs. *PLoS One* **13**, e0189792 (2018).
16. K. S. Rodgers, K. D. Bahr, P. L. Jokiel, A. Richards Donà, Patterns of bleaching and mortality following widespread warming events in 2014 and 2015 at the Hanauma Bay Nature Preserve, Hawai'i. *PeerJ* **5**, e3355 (2017).
17. M. Winston *et al.*, "Preliminary Results of Patterns of 2019 Thermal Stress and Coral Bleaching across the Hawaiian Archipelago" (NOAA Administrative Rep. H-20-04, NOAA, Washington, DC, 2020).
18. G. P. Asner *et al.*, Large-scale mapping of live corals to guide reef conservation. *Proc. Natl. Acad. Sci. U.S.A.* **117**, 33711–33718 (2020).
19. M. P. Lesser, J. H. Farrell, Exposure to solar radiation increases damage to both host tissues and algal symbionts of corals during thermal stress. *Coral Reefs* **23**, 367–377 (2004).
20. S. A. Foo, G. P. Asner, Scaling up coral reef restoration using remote sensing technology. *Front. Mar. Sci.* **6**, 79 (2019).
21. S. A. Foo, G. P. Asner, Impacts of remotely sensed environmental drivers on coral outplant survival. *Restor. Ecol.* **29**, e13309 (2021).
22. T. P. Hughes *et al.*, Spatial and temporal patterns of mass bleaching of corals in the Anthropocene. *Science* **359**, 80–83 (2018).
23. R. Ritson-Williams, R. D. Gates, Coral community resilience to successive years of bleaching in Kāne'ohe Bay, Hawai'i. *Coral Reefs* **39**, 757–769 (2020).
24. J. Gove *et al.*, Coral reef benthic regimes exhibit non-linear threshold responses to natural physical drivers. *Mar. Ecol. Prog. Ser.* **522**, 33–48 (2015).
25. J. M. Gove *et al.*, Near-island biological hotspots in barren ocean basins. *Nat. Commun.* **7**, 10581 (2016).
26. W. Fitt, B. Brown, M. Warner, R. Dunne, Coral bleaching: Interpretation of thermal tolerance limits and thermal thresholds in tropical corals. *Coral Reefs* **20**, 51–65 (2001).
27. K. Cawse-Nicholson *et al.*, NASA's surface biology and geology designated observable: A perspective on surface imaging algorithms. *Remote Sens. Environ.* **257**, 112349 (2021).
28. G. P. Asner *et al.*, Carnegie Airborne Observatory-2: Increasing science data dimensionality via high-fidelity multi-sensor fusion. *Remote Sens. Environ.* **124**, 454–465 (2012).
29. G. P. Asner, N. R. Vaughn, C. Balzotti, P. G. Brodrick, J. Heckler, High-resolution reef bathymetry and coral habitat complexity from airborne imaging spectroscopy. *Remote Sens.* **12**, 310 (2020).
30. G. P. Asner *et al.*, Abiotic and human drivers of reef habitat complexity throughout the Main Hawaiian Islands. *Front. Mar. Sci.* **8**, 90 (2021).
31. E. Maturi *et al.*, A new high-resolution sea surface temperature blended analysis. *Bull. Am. Meteorol. Soc.* **98**, 1015–1026 (2017).
32. NOAA Coral Reef Watch, NOAA Coral Reef Watch Version 3.1 Daily Global 5km Satellite Coral Bleaching Degree Heating Week Product (Version 3.1, NOAA, Washington, DC, 2021).
33. J. M. Gove *et al.*, Quantifying climatological ranges and anomalies for Pacific coral reef ecosystems. *PLoS One* **8**, e61974 (2013).
34. M. K. Donovan *et al.*, Local conditions magnify coral loss after marine heatwaves. *Science* **372**, 977–980 (2021).
35. S. Sully, R. van Woesik, Turbid reefs moderate coral bleaching under climate-related temperature stress. *Glob. Change Biol.* **26**, 1367–1373 (2020).
36. G. J. Huffman, E. F. Stocker, D. T. Bolvin, E. J. Nelkin, J. Tan, "GPM IMERG Final Precipitation L3 1 month 0.1 degree x 0.1 degree V06" (Rep., Goddard Earth Sciences Data and Information Services Center [GES DISC], Greenbelt, MD, 2019). https://doi.org/10.5067/GPM/IMERG/3B-MONTH/. Accessed 4 April 2022.
37. K. Falinski, *Predicting Sediment Export into Tropical Coastal Ecosystems to Support Ridge to Reef Management* (University of Hawaii at Manoa, 2016).
38. R. B. Whittier, A. I. El-Kadi, "Human and environmental risk ranking of onsite sewage disposal systems for the Hawaiian islands of Kauai, Molokai, Maui, and Hawaii" (Rep., Department of Geology and Geophysics, School of Ocean and Earth Science and Technology, University of Hawaii at Manoa, Manoa, HI, 2014). http://hdl.handle.net/10125/50771. Accessed 4 April 2022.
39. N. Li *et al.*, Thirty-four years of Hawaii wave hindcast from downscaling of climate forecast system reanalysis. *Ocean Model.* **100**, 78–95 (2016).
40. L. Breiman, Random forests. *Mach. Learn.* **45**, 5–32 (2001).
41. F. Pedregosa *et al.*, Scikit-learn: Machine learning in python. *J. Mach. Learn. Res.* **12**, 2825–2830 (2011).
42. G. P. Asner, N. Vaughn, J. Heckler, Global Airborne Observatory: Hawaiian Islands live coral cover 2020. Zenodo. https://doi.org/10.5281/zenodo.4777345. Deposited 15 April 2022.